Evaluating Thera-101 as a Low Volume Resuscitation Adjunct in a Model of Traumatic Brain Injury and Hemorrhage

Jessica Stukel Shah
Naval Medical Research Unit San Antonio
Joseph Macaitis
Naval Medical Research Unit San Antonio
Bridney Lundquist
Naval Medical Research Unit San Antonio
Brian Johnstone
Theratome Bio, Inc
Michael Coleman
Theratome Bio, Inc
Michelle Jefferson
Air Force Research Laboratory, 711th Human Performance Wing
Jacob Glaser
Naval Medical Research Unit San Antonio
Annette Rodriguez
Naval Medical Research Unit San Antonio
Sylvain Cardin
Naval Medical Research Unit San Antonio
Heuy-Ching Wang (heuy-ching.h.wang.civ@mail.mil)
Naval Medical Research Unit San Antonio
Alexander Burdette
Naval Medical Research Unit San Antonio

Article

Keywords: Secretome, cell-based therapy, trauma, neuroprotection, organ damage

Posted Date: May 26th, 2022

DOI: https://doi.org/10.21203/rs.3.rs-1609940/v1

Abstract

Traumatic brain injury (TBI) and hemorrhage remain challenging to treat in austere conditions. Developing a therapeutic to mitigate the associated pathophysiology is critical to meet this treatment gap, especially as these injuries and associated high mortality are possibly preventable. Here, Thera-101 (T-101) was evaluated as an adjunct to low volume resuscitation in a rat model of TBI and hemorrhage. The therapeutic, T-101, is uniquely situated as a TBI and hemorrhage intervention. It contains a cocktail of proteins and microvesicles from the secretome of adipose derived mesenchymal stem cells that can act on numerous mechanisms associated with poly-trauma. T-101 efficacy was determined at four, 24, 48, and 72 hours after injury by evaluating blood chemistry, inflammatory chemo/cytokines, histology, and diffusion tensor imaging. Blood chemistry indicated that T-101 reduces markers of liver damage to Sham levels while the levels remain elevated with the vehicle control. Histology supports the potential protective effects of T-101 on the kidneys. Diffusion tensor imaging shows that the injury caused the most damage to the corpus callosum and the fimbria. Immunohistochemistry suggests that T-101 may mitigate astrocyte activation at 72 hours. Together, these data suggest T-101 could be a potential field deployable adjunct for low volume resuscitation.

Introduction

Poly-trauma including hemorrhage and traumatic brain injury (TBI) is a leading cause of morbidity and mortality in both the civilian and military settings. In the civilian setting, 26% of trauma patients with a severe brain injury also presented with hemorrhagic shock[1]. In the military setting, explosions accounted for 72% of those who died from wounds in Operation Iraqi Freedom and Operation Enduring Freedom. The majority of those cases included the deadly combination of TBI (83%) and hemorrhage (16%). In that population, 80% of potentially survivable injuries were due to hemorrhage, with TBI present in 9% of those injuries[2]. Together these injuries comprise a major focus to improve available therapeutics from the point of injury through prolonged field care.

It is known that TBI worsens outcomes and increases mortality in patients also experiencing hypotension and shock[3]. A clinical study determined that the mortality rate of patients with head injury increased from 45–83% during the first 24 hours when shock was present[4]. A potential reason for this increase to occur may be that poly-trauma with TBI and hemorrhage results in metabolic destabilization, acidosis, inflammation, organ injury and failure, neurological dysfunction, and neuronal death[5,6]. Throughout prolonged field care, the consequences of such injuries may worsen without appropriate therapeutics to mitigate the pathophysiology associated with extended resuscitation when lacking whole blood or blood products. Thus, approaches for metabolic and tissue stabilization to enable prolonged pre-hospital survivability are necessary.

The recommended resuscitation guidelines from the Brain Trauma Foundation for patients with TBI calls for a systolic blood pressure (SBP) > 100mm Hg for patients age 50–69, and > 110mm Hg for patients 15–49 years old and > 70 years old[7]. The 2020 Tactical Combat Casualty Care Guidelines for Medical

Personnel calls for maintaining a SBP of 100-100mm Hg in a casualty with an altered mental status due to suspected TBI. The required focus on brain protection using aggressive fluid resuscitation can produce deleterious effects including end organ damage and induction of systemic inflammatory response syndrome, which lessens the overall recovery from poly-trauma[8,9]. Unfortunately, no therapeutic strategy exists to target the numerous cellular pathways involved in poly-trauma as many FDA approved drugs only have a single target (e.g. antibodies, chemical inhibitors, and single growth factors such as platelet-derived growth factor). Thus, there is a need for novel or improved methods for the resuscitation and stabilization of casualties with combined hemorrhage and acute TBI with or without multiple trauma.

Mesenchymal stem cell (MSC)-based therapeutics represent a promising strategy for addressing combat-related poly-traumatic injuries due to their demonstrated beneficial effects in treating many disease indications in preclinical and early clinical studies[10,11]. However, cellular therapies are not practical in the pre-hospital environment due to requirements for ultra-low storage temperatures, relatively long processing times to ensure cell viability, and adequate removal of cryoprotectants. Additionally, potency of direct MSC administration is variable and the therapeutic effect might be delayed long after administration, which further limits their value in acute trauma. It is increasingly recognized that the MSC secretome, also termed paracrine factors or conditioned medium, is responsible for the majority of beneficial effects observed with MSCs in various disease models and early clinical trials[12,13]. Secretome trophic factor components interact cooperatively to regulate multiple endogenous reparative and protective pathways, and in at least one case synergistically[14]. In addition to freely soluble therapeutic protein factors, the secretome contains microvesicles (e.g. exosomes) that encapsulate protein factors, nucleic acids (e.g. miRNA) and metabolites with demonstrated therapeutic benefits[15,16]. Adipose-derived mesenchymal stem cells (ASC), and specifically the secretome products, have beneficial properties that have shown reduced inflammation and lung injury while enhancing endothelial protection. Furthermore, ASC secretome products revealed improved metabolic stabilization and cell survival, reduced liver, kidney, and muscle damage, as well as enhanced neuronal survival and protection against brain injury[17–21]. These beneficial effects on multiple tissues and organs suggest that the MSC secretome could be a valuable point-of-injury therapeutic following TBI and hemorrhage.

Thera-101 (T-101) is a novel ASC secretome-based therapeutic developed by Theratome Bio, Inc. that is free of animal components and offers several potential competitive advantages over cellular therapy. The product is a liquid stored at below-20°C with a prototype lyophilized formulation in development, which would further ease administration in the pre-hospital environment. Additionally, T-101 contains a combination of freely soluble exosome-associated factors that have critical therapeutic activity including hepatocyte growth factor (HGF), vascular endothelial growth factor (VEGF), brain-derived neurotrophic factor (BDNF), nerve growth factor (NGF), and glial-derived neurotrophic factor (GDNF)[14,19,22,23]. Importantly, a previous study showed that administration of T-101 was effective in mitigating injury in a rat model of brain hypoxia-ischemia, leading to long-term improvements in motor and cognitive functions[22]. Thus, the beneficial properties of T-101 make it a promising candidate as an adjunct to resuscitative therapy following TBI and hemorrhage.

In this study, T-101 was investigated in a poly-trauma rodent model of TBI and 35% volume-controlled hemorrhage to determine its efficacy in preventing and/or mitigating end organ damage, inflammation, and brain injury. Specifically, the effects of T-101 on systemic inflammation and liver, kidney, muscle, lung, and brain damage were evaluated. If effective, T-101 has the potential to treat potentially survivable injuries in the military and civilian setting for patients experiencing poly-trauma.

Materials And Methods

Rat Poly-trauma Model

The study protocol was approved by the Institutional Animal Care and Use Committee at the 711th Human Performance Wing, Joint Base San Antonio-Fort Sam Houston, in compliance with all applicable Federal regulations governing the protection of animals in research. The study is reported in accordance with ARRIVE guidelines. The experiments reported herein were conducted in compliance with the Animal Welfare Act and per the principles set forth in the “Guide for Care and Use of Laboratory Animals,” Institute of Laboratory Animals Resources, National Research Council, National Academy Press, 2011.

Male, Sprague Dawley rats (290-325g) acquired from Charles River Laboratories (Frederick, MD) were acclimated to the facility for at least seven days. Subjects were pair-housed upon arrival and single-housed following the procedure on a 12-hour light/dark cycle with ad libitum access to food and water. Food and hydration support were placed on the floor of the cage following the procedure to ensure easy access during recovery. Each subject was induced with 3-3.5% isoflurane and administered a pre-operative dose of Buprenorphine HCl (0.1mg/kg) (Reckitt Benckiser Healthcare, Slough, Berkshire). Anesthesia was maintained at 0.5-2% isoflurane and rats were placed on a physiological monitoring system (Harvard Apparatus, Holliston, MA) that regulated body temperature and recorded heart rate (HR), oxygen saturation (SpO_2), systolic and diastolic blood pressure, and respiration rate (RR).

The procedure timeline is depicted in Fig. 1. First, vascular access was obtained by cannulating the femoral artery and vein with heparin coated polyethylene (PE)-50 tubing (Instech Laboratories, Inc, Plymouth Meeting, PA) and a rat femoral vein catheter (Instech Laboratories, Inc, Plymouth Meeting, PA), respectively. Mean arterial pressure (MAP) was monitored with a pressure transducer (Micro-Med INC, Louisville, KY) and Blood Pressure Analyzer (Micro-Med INC, Louisville, KY) from the arterial line. The rat was moved to the prone position and a round metal disc (10mm diameter by 3mm thick) (online metals.com, Seattle, WA) was centered and secured on the subject’s head using tissue glue. A 10-minute stabilization period followed, then pre-injury vitals were recorded (Supplemental 1). Next, the electrocardiogram leads and the SpO_2 sensor were removed, the catheter lines were closed, and the subject was transferred to the TBI device consistent with the Marmarou weight drop model[24]. The device consisted of a platform with a 1.8m long clear plastic guide tube (22.23mm outer diameter, 15.88mm inner diameter) through which a 450g brass weight fell freely. A foam bed (type E, Foam to Size, Ashland, VA) was positioned inside a plexiglass container under the guide tube. TBI was induced by dropping the weight through the guide tube to allow contact with the metal disc on the rat’s head from a height of

1.25m[24]. A velocity sensor (TDS 3054B, Tektronix, Beaverton, OR) was used to ensure consistent velocity of the weight near the bottom of the guide tube was achieved for each subject (5.0 ± 0.5mm/s). Following the TBI, the rodent was quickly transferred to the physiological monitoring system, the catheters were reconnected, and the ECG leads and SpO_2 sensor were placed. Isoflurane was maintained at 1% for the duration of the procedure.

After obtaining a post-TBI MAP recording, the 35% volume-controlled hemorrhage was induced using a programmable syringe pump (Legato 110, KD Scientific, Holliston, MA) at a withdrawal rate of 1mL/min from the arterial catheter. The hemorrhage volume was calculated from the total estimated blood volume for rats at 64mL/kg[25]. The MAP was recorded immediately following the hemorrhage then monitored continuously throughout the remainder of the surgical procedure. Next, resuscitation was initiated 15 minutes after the start of hemorrhage[26]. Subjects were randomly assorted into groups to receive the vehicle control or T-101 with terminal end points at four, 24, 48, or 72 hours after the start of hemorrhage (n = 5/group at each time-point). The number of animals used in this study was determined based on previous reports of brain and organ injury in rat models of TBI + hemorrhage[21,27]. A 1mL bolus of vehicle control (saline) or T-101 (1.7mg/kg) was administered through the venous catheter using a T-101 dosage based on previous mouse stroke data[28]. An additional 0.5mL saline was infused at 0.1ml/min if the MAP did not reach 70mmHg within five minutes of the bolus. Therefore, the maximum resuscitation volume was 1.5mL per rat and resuscitation was completed within 10 minutes of the bolus. After resuscitation, the cannulated vessels were ligated, catheters and leads were removed, and a post-operative dose of Buprenorphine SR (1.0mg/kg) (Zoopharm, Fort Collins, CO) was administered. The animal was returned to a fresh cage for post-surgical monitoring until the endpoint was reached. Shams underwent all surgical preparation and were maintained under anesthesia for a period of time consistent with the vehicle control and T-101 groups, but they did not experience the TBI or hemorrhage. The subjects were monitored for 72 hours following the estimated time when hemorrhage would have been initiated, and then euthanized at the 72-hour time-point with final blood collection and tissue harvesting at that 72-hour time-point.

At the assigned endpoint, all animals were placed under deep isoflurane anesthesia, given a dose of Buprenorphine HCl (0.1mg/kg), and transcardial perfusion was performed as previously described[29]. A final blood draw was obtained immediately before the perfusion from the left ventricle and transferred to blood collection tubes with lithium heparin or ethylenediaminetetraacetic acid (EDTA) for blood chemistry or multiplexed analyte quantification, respectively. The perfusion was performed using the Leica Perfusion Two™ automated perfusion system (Leica Biosystems, Buffalo Grove, IL) according to the manufacturer's instructions by first infusing 10% sucrose to clear the blood, followed by 10% formalin for fixation.

Histopathology of Lung, Kidney, and Liver

The lungs, kidneys, and liver were transferred to 10% buffered formalin for at least 72 hours and then embedded in paraffin (Fisherbrand Histoplast™ PE, Pittsburg, PA). They were then sectioned to 5–6μm thickness, and stained with hematoxylin and eosin (H&E) stain (Hematoxylin+, Thermo Fisher Scientific,

Pittsburg, PA; Eosin-Y Alcoholic 0.25%, Stat Lab Medical Products, McKinney, TX). One section per block was imaged and scored by a board certified veterinary pathologist. Scores were assigned on a scale of 0–5 to indicate the severity or degree of histologic finding present in examined tissue: 0 (not present), 1 (minimal), 2 (mild), 3 (moderate), 4 (marked), or 5 (severe). Cells were scored by the following scale: 0: negative, 1: <10% of cells in section are affected (minimal), 2: 11–25% of cells in section are affected (mild), 3: 26–50% of cells in section are affected (moderate), 4: 50%-75% of cells in section are affected (marked), and 5: >75% of cells in section are affected (severe).

Immunohistochemistry and Diffusion Tensor Imaging

For brain analysis, the subject's head was fixed in 10% buffered formalin for 72 hours then transferred to phosphate buffered saline (PBS) containing 0.01% sodium azide for shipment to Biospective Inc. (Montreal, Canada) for *ex vivo* diffusion tensor imaging (DTI) and immunohistochemistry. Scientists at Biospective Inc. remained blinded to the treatment group during data collection and analysis. Each brain specimen was evaluated by Magnetic resonance imaging (MRI, 7T Bruker BioSepc 70/30 system, Bruker Biospin, Ettlingen, Germany). Samples were placed in the scanner and warmed to 44°C ± 0.3°C. Multi-dimensional, multi-shell images were obtained in 50 directions with three shells and six b0 images. The MRI images were processed with NIGHTWING™ software (Biospective Inc, Montreal, Canada). The lowest shell was removed from analysis due to ringing artifact. Each reconstructed image was corrected for non-uniformity with the N3 algorithm[30], brain masking, and linear spatial normalization with a 12-parameter affine transformation to map individual images from a native coordinate space to a reference space. Next, an unbiased, symmetric, anatomical template was generated from the b0 images[31,32] and images were linearly and nonlinearly registered to this anatomical template[31,33,34]. Image segmentation was achieved by identifying neuroanatomical regions on the atlas. DTI parametric maps were generated with an automated method to compute mean diffusivity (MD), axial diffusivity (AD), radial diffusivity (RD), and fractional anisotropy (FA). The parametric maps were then mapped into the template space.

Following MRI, the brain tissue was prepared for immunohistochemistry. The brain specimens were extracted from the skull and processed for paraffin embedding. Blocks were sectioned coronal in orientation at a thickness of 5µm to target the anterior, middle, and posterior segments of the corpus callosum, overlying cortex, hippocampus, and fimbria. All sections were stained with cresyl violet to label the Nissl substance in neurons and immunostained for glial fibrillary acidic protein (GFAP) to label astrocytes. First, sections were de-paraffinized and rehydrated. The cresyl violet stain was prepared as a 0.1% stock of cresyl violet acetate (Sigma-Aldrich C5042) in deinonized water. Ten drops of 10% acetic acid were added to a 30mL stock solution for each round of staining. Slides were stained for three minutes, then dehydrated and mounted with Permount mounting medium. GFAP staining was performed on a Lab Vision 360 Autostainer (Fisher Scientific, Toronto, Canada) with detergent reagents from Abcam. The slides underwent epitope retrieval by incubating them in citrate buffer (pH 6.0) and heating to 120°C under high pressure for 10 minutes. Endogenous peroxidase was quenched by sequential incubations in hydrogen peroxide for five minutes. Next, the slides were incubated in Protein Block (Abcam ab156024) for five minutes followed by 60 minutes with the primary antibody (rabbit Ab anti-GFAP, Thermo Fisher

RB-087-A; 1:100). The secondary antibody (donkey anti-rabbit IgG [Jackson ImmunoResearch] and Streptavidin-HRP [Abcam ab64269]) conjugate was added for tissue visualization using AEC Single Solution (Abcam ab64252) for 20 minutes. The sections were counterstained with Acid Blue 129 (Sigma-Aldrich, St. Louis, MO) and mounted with aqueous mounting medium[35]. The stained sections were digitalized on an Axio Scan.Z1 digital whole slide scanner (Carl Zeiss, Canada). Image processing involved manually delineating regions of interest and using the automated PERMITS™ quantification process to determine the percent positive-stained area.

Laboratory Assays

Blood plasma collected in lithium heparin tubes were used for blood chemistries. The IDEXX Catalyst One Analyzer (IDEXX, Westbrook, Maine) clips included creatinine (CREA), creatine kinase (CK), alanine aminotransferase (ALT), aspartate aminotransferase (AST), lactate (LAC), and lactate dehydrogenase (LDH). Blood plasma specimens collected in EDTA tubes were evaluated for inflammatory markers. Initially, a 27-plex assay was evaluated to identify detectable analytes to down-select. Next, a customized rat four-plex cytokine/chemokine kit (Millipore, Burlington, MA) on a Bio-plex® 200 Luminex system (Bio-Rad, Hercules, CA) was used for analyses according to manufacturer's instructions based on the analytes that had detectable levels from the 27-plex assay. The custom kit included interleukin (IL)-1β, IL-6, inflammatory protein-10 (IP-10), and leptin.

Statistical Analysis

Data are plotted as mean ± standard deviation and statistics were run on GraphPad Prism 8.3 (GraphPad Software, San Diego, CA) with $P < 0.05$ considered to be statistically different. Vitals data were analyzed with repeated measures ANOVA. The analysis for blood chemistry, luminex, histology and brain assessment was performed on n = 5 rats/group which survived to their end-point. Log-transformed blood chemistry and inflammation data were analyzed with a one-way ANOVA comparing injury groups and the Sham group, with Bonferroni's multiple comparison test. Histological assessment scores were analyzed for each group compared to the Sham group via the one-way ANOVA Kruskal-Wallis test with Dunnet's multiple comparisons post hoc test. All brain analysis data were analyzed using a one-way ANOVA and Bonferroni's multiple comparison test. Voxel-wise statistical analysis of the DTI maps were completed using the SurfStat toolbox. The p-values without correction for multiple comparisons were reported and $P < 0.05$ were considered significant.

Results

Survival and Vitals

The first eight hours following injury were the most critical with the greatest drop in survival. If an animal made it through this period, it was likely they would survive to their end- point. Eight subjects expired prior to resuscitation and therefore were excluded from the study. Of these, three expired following the TBI, one expired during the hemorrhage, and the remaining four subjects expired after the hemorrhage. No

incidence of skull fracture was observed. For the rats that survived through completion of resuscitation, the survival rates remained consistent for the vehicle control and T-101 groups with no significant differences between groups over time data not shown). The Sham group had no mortality.

Vitals including heart rate, MAP, SpO_2, and respiration rate were monitored throughout the procedure and are listed in Table 1 (Supplemental 1). As expected, MAP dropped following hemorrhage by 30-35mmHg from Pre-injury. Vehicle and T-101 fluids returned the MAP to Pre-injury levels following the resuscitative bolus. The respiration rate increased after the TBI and returned to Pre-injury levels by the time the hemorrhage was complete. Changes in heart rate and SpO_2 occurred throughout the procedure but did not reach significance. Significant differences from Pre-Injury are noted in bold text. The animal was recovered and free to move about the cage following resuscitation so vitals were not monitored throughout the recovery period.

Plasma Markers of Organ Damage and Inflammation

Blood chemistry was measured from plasma for the Sham group and injury groups at four, 24, 48, and 72 hours after the start of hemorrhage (Fig. 2). Elevated plasma AST and ALT served as markers of liver damage, elevated CK was indicative of muscle damage, elevated LDH was indicative of cell death, elevated CREA was indicative of kidney damage, and elevated LAC was indicative of activation of anaerobic metabolism. The levels of ALT significantly (*$P < 0.05$) increased compared to the Shams (54.8 ± 2.59) by 2.3-fold at 24 hours in the vehicle control group (123.4 ± 45.73), while the T-101 group maintained ALT (4hr: 61.0 ± 15.44; 24hr: 78.2 ± 31.80; 48hr: 64.2 ± 33.80; 72hr: 60.8 ± 16.74) near Sham levels at each time point. AST levels increased significantly ($P < 0.05$; 689.4 ± 299.29) at 24hr in the vehicle control group compared to the T-101 group (306.4 ± 169.61) and Sham group. (54 ± 7.48) LDH peaked initially at four hours in the T-101 group (though not significantly), and declined through 72 hours. In the vehicle control group, LDH levels significantly increased at 24hr ($P < 0.05$; 1455.8 ± 822.06) compared to Shams (293.2 ± 189.09). Both groups returned to near Sham levels by 72 hours. LAC levels were not significantly altered between groups. Plasma was also sampled to analyze systemic inflammation using the Luminex multiplex protein technology at four, 24, 48, and 72 hours after the start of hemorrhage (Fig. 3). No significant differences between groups were noted for leptin, IL-6, IL-1β, or IP-10.

Histopathological Analysis of Organ Injury

The liver, kidney, and lung were evaluated by H&E staining to determine if T-101 mitigated organ damage compared to the vehicle control. Parameters with significant differences from Shams are identified with bold text in Table 2 (Supplemental 2). Overall, the results indicated that T-101 imparted noted kidney protection (Fig. 4). Specifically, renal necrosis was greater in the vehicle control group at 24hr (1.0 ± 0.9) compared to subjects that received T-101 (0.1 ± 0.3). Additionally, the vehicle control group exhibited tubular degeneration that was significantly higher ($P < 0.0005$; 2.7 ± 0.5) than the sham group (0.00 ± 0.0) at 48hr, while T-101 was minimally altered (0.09 ± 0.7). Effects on the liver were time dependent with both

groups exhibiting mild to moderate hepatic necrosis at four hours; Although the T-101 liver histopathology (dilation/fibrin and congestion) score showed a significant increase at four hours (##P< 0.005; 1.6 +- 0.5) compared to the vehicle control group, the T-101 histopathology score returned to Sham levels (0.0 ± 0) by 48 hours. Additionally, liver necrosis histopathology scores were consistently lower than the vehicle control at all time-points. Examination of the lungs showed that the vehicle control group exhibited perivascular edema at significantly higher levels (P< 0.05; 1.8 ± 0.8) compared to the Sham group (0.00 ± 0) at 24 hours, and continued to increase with significance observed again at 72 hours (P< 0.005; 2.0 ± 0.7), compared to Shams. The T-101 group exhibited a significant increase (P< 0.005; 2.8 ± 01.1) of perivascular edema at 4 hours compared to Shams, which decreased to non-significant levels from 24 to 72 hours. No significant differences between vehicle control and T-101 were noted at any time-point.

Evaluating the Neuroprotective Effects of T-101

The neuroprotective effects of T-101 were evaluated by DTI and immunohistochemistry. First, the brain was scanned by MRI to obtain DTI maps. Fractional anisotropy (FA) was calculated from these DTI maps and lower values are indicative of injury with water diffusion in a direction other than along neuronal tracks. The greatest difference from the Sham group was observed for FA in the corpus callosum followed by the fimbria (Fig. 5). In the corpus callosum, FA for the vehicle control was greater than T-101 at 24 and 72 hours. This effect was reversed at 48 hours, but there was also greater variability between subjects. The second most affected region of the brain was the fimbria. Similar to the corpus callosum, the greatest number of differences were noted in FA compared to the other DTI parameters, axial, radial, and mean diffusivity.

Brain immunohistochemistry showed similar results between the Sham and injury groups in the corpus callosum and overlying cortex, as well as the fimbria (Fig. 6). The lack of significant differences could be due to the large variation within groups. Although not significant, GFAP staining in the corpus callosum and fimbria of the T-101 group is trending below the vehicle control group from 24 to 72 hours, with about 50% reduction from the T-101 mean compared to the vehicle control. The representative images show more densely stained astrocytes with a bushy morphology at these time-points, indicating that T-101 may be mitigating astrocyte activation and potential neuro-inflammation. In the hippocampus, there is increased Nissl substance for the T-101 group, compared to the Sham group and the vehicle control at 48 hours. By 72 hours, the GFAP staining density of the vehicle control group in the hippocampus is much more than the T-101 group, although not significant.

Discussion

As prolonged field care is expected in future conflicts, effective adjuncts for low volume resuscitation are critical to support our warfighters in far forward, resource-constrained environments. This report evaluated T-101, a therapeutic derived from the ASC secretome, to address this current gap. One goal of this study was to evaluate the ability for T-101 to reduce or mitigate organ damage. Blood chemistry

results demonstrated that the model induced damage to the liver and muscle tissue as well as increased cell death at four or 24 hours. Of these, T-101 had potential protection for the liver based on the blood chemistry. Comparable trends in AST and ALT were observed in a similar injury model indicating that liver damage is common in poly-trauma with TBI and hemorrhage and therefore a focus for evaluating efficacy of therapeutics[27]. Banas et al. reported that ASC whole cell grafts improved liver function following injury and these benefits were attributed to secreted NGF, HGF, and VEGF[19]. It follows that T-101, abundant in these factors, would serve as a promising alternative while reducing the burdens of direct cell administration. The most significant finding of the H&E staining results is the indication that T-101 may provide protection to the kidneys, especially after 48 hours. Histology results were similar to Ronn et al. who reported pathological changes to the kidney, liver, and small intestine, but the lungs remained unaffected[36]. Chen et al. also reported ASCs protected kidneys in an ischemia-reperfusion model by lowering oxidative stress and the inflammatory reaction[20]. Overall, the data suggests the potential robustness of secretome-based therapeutics to target multiple organs in a single drug.

The brain was evaluated by DTI and immunohistochemistry to evaluate injury severity and effects of T-101. First, DTI was utilized as a tool to quantify brain injury, specifically which attributed to diffuse axonal injury as is expected in this model. The degree of anisotropy in water diffusion along neuronal tracts in the brain revealed that the corpus callosum and fimbria were the most affected regions of the brain. Decreasing FA values indicate an injury, either due to dying neurons, damaged axons, or the surrounding myelin because the water diffusion has shifted to a radial plane[37 38]. In our study, we found no positive effects of T-101 on mitigating brain injury from TBI. Others have demonstrated the strong potential for a secretome-based therapy to mitigate brain damage as both the conditioned medium from ASCs and the cell-based therapy improved motor and cognitive function in 6-month-old rats[21]. It is possible a larger dose of T-101 may be needed to mitigate brain injury from TBI.

Second, immunohistochemistry for each of the brain regions analyzed in this study showed changes after injury. Increased GFAP staining in the hippocampus as well as the bushy morphology and dense cell body suggest increased activation. While GFAP staining with T-101 treatment was generally less than the vehicle control groups, it was not statistically significant. Similar trends were also observed in the corpus callosum and fimbria. T-101 could be reducing astrocyte activation in these regions, but due to the high variability, it was not statistically significant. Together, the imaging techniques to evaluate the injury model and effects of T-101 showed trends toward lower astrocyte activation with T-101 treatment, but it is likely a higher dosage may be required for more clinically relevant differences. Outcomes were similar to other published reports on damage to the corpus callosum in TBI models[40]. The corpus callosum is the primary commissural region of the brain; the white matter tracts connecting the right and left hemispheres are responsible for transferring sensory, motor, and high-level cognitive signals[41]. Additionally, as the hippocampus is responsible for learning and memory, mitigating damage could have profound impacts on patient health[42]. Therefore, identifying a therapeutic that mitigates damage, particularly in this region of the brain, has the potential for significant clinical success.

We also assessed the potential impact of injury and T-101 on systemic inflammation over the course of 72 hours. In our model, multiplexed analysis of inflammatory markers did not show a significant increase in leptin, IL-6, IL-1β, or IP-10 at any time-point. These analytes were selected from a 27-plex inflammation panel as they resulted in detectable levels (data not shown) from initial pilot studies. In a similar injury model from a previous report, the treatment group also demonstrated similar IL-6 levels to shams four hours after injury, but levels were elevated in the vehicle control group[27]. In contrast, Xu et al. used a TBI rodent model followed by secretome dosing through Day 7 that demonstrated reduced inflammation and apoptosis with a noted change in microglia phenotypes from M1 cells (inflammatory) to M2 cells [anti-inflammatory]. Inflammatory and anti-inflammatory mediators were evaluated through Day-14 post-TBI[43]. A separate study revealed ASC conditioned media enhanced protective neurovascular modulation in a mild traumatic brain injury model[44]. Consistency with Sham levels in our model could be due to the time-points when blood was collected, or it could suggest that a more severe model might be necessary to observe this effect often associated with poly-trauma. As the Sprague Dawley rats are an outbred strain, some variability is expected and could have attributed to the standard deviation with groups.

In addition to the above-mentioned benefits of T-101, the ease of transitioning this therapeutic to the clinic is a significant advantage. T-101 is manufactured under good manufacturing practices (GMP), which ensures stringent quality control measures are maintained for safe and consistent drug production. Another benefit of secretome-based therapeutics is the numerous factors encompassed in a single drug; however, few report quantified levels of these factors so direct comparison between studies remains challenging. These factors have been defined and proven to be consistent across lots in T-101. As it is derived from human cells, there is a lesser gap when transitioning to clinical studies than with animal derived treatments. Therefore, risks associated with successful clinical transition are reduced.

Overall, results indicate T-101 may have the potential to serve as a protective agent to reduce liver and kidney organ damage based on the reduced AST and ALT levels, and improved viability of renal cells compared to vehicle controls based on pathology analysis. Further investigations and formulation refinement will be required however, to continue to probe the systemic response and establish the optimal dosing and formulation regimen in a model of increased severity. A lyophilized formulation of T-101 is in development, which allows for a field deployable therapeutic without < 0°C storage conditions. Further refinement and formulation optimization of this therapeutic could provide first responders with an intervention to treat poly-trauma injuries, and has the possibility to improve outcomes of potentially survivable injuries.

Declarations

Acknowledgements

This work is funded by Joint Program Committee-6 (JPC-6) using work unit number G1811.

The study protocol was reviewed and approved by the 711th HPW/RDH JBSA-Fort San Houston Institutional Animal Care and Use Committee in compliance with all applicable Federal regulations governing the protection of animals in research. The experiments reported herein were conducted in compliance with the Animal Welfare Act and per the principles set forth in the "Guide for Care and Use of Laboratory Animals," Institute of laboratory Animals Resources, National Research Council, National Academy Press, 2011.

Author Contributions

JSS performed the experiments, analyzed data, designed the figures and wrote the manuscript. BL and JM performed the experiments, collected, analyzed data, and contributed to editing the manuscript, MAJ conducted the histopathological analyses, ARR analyzed data, designed the figures, and contributed to writing the manuscript; HCW analyzed data, supervised the project, and contributed to editing the manuscript, SC supervised the project and contributed to editing the manuscript; JG, BJ and MC developed the project; AB developed the project, designed the research and wrote the manuscript; and all authors provided critical feedback and helped shape the research and manuscript.

Additional Information

Correspondence and request for materials should be addressed to AB and HCW.

The datasets generated and/or analysed during the current study are available from the corresponding authors upon request.

Competing Interests Statement. MC is the CEO of TheratomeBio (Thera-101 developer/manufacturer). BJ is affiliated with TheratomeBio.

The remaining authors (JSS, JM, BL, MAJ, JG, ARR, SC HCW, and AB) have no competing interests.

References

1. Mayer, A. R. *et al.* A systematic review of large animal models of combined traumatic brain injury and hemorrhagic shock. Neurosci Biobehav Rev **104**, 160–177, doi:10.1016/j.neubiorev.2019.06.024 (2019).
2. Eastridge, B. J. *et al.* Died of wounds on the battlefield: causation and implications for improving combat casualty care. J Trauma **71**, S4-8, doi:10.1097/TA.0b013e318221147b (2011).

3. Mclaughlin A. Traumatic Brain Injury in the Military. Open Journal of Modern Neurosurgery. **3**, 23–28, doi:10..4236/ojmn.2013.32005. (2013).
4. Manley, G. *et al.* Hypotension, hypoxia, and head injury: frequency, duration, and consequences. Arch Surg **136**, 1118–1123, doi:10.1001/archsurg.136.10.1118 (2001).
5. Gann, D. S. & Drucker, W. R. Hemorrhagic shock. J Trauma Acute Care Surg **75**, 888–895, doi:10.1097/TA.0b013e3182a686ed (2013).
6. Werner, C. & Engelhard, K. Pathophysiology of traumatic brain injury. Br J Anaesth **99**, 4–9, doi:10.1093/bja/aem131 (2007).
7. Rauch, S. *et al.* Severe traumatic brain injury and hypotension is a frequent and lethal combination in multiple trauma patients in mountain areas - an analysis of the prospective international Alpine Trauma Registry. Scand J Trauma Resusc Emerg Med **29**, 61, doi:10.1186/s13049-021-00879-1 (2021).
8. Chesnut, R. M. *et al.* The role of secondary brain injury in determining outcome from severe head injury. J Trauma **34**, 216–222, doi:10.1097/00005373-199302000-00006 (1993).
9. Chatrath, V., Khetarpal, R. & Ahuja, J. Fluid management in patients with trauma: Restrictive versus liberal approach. J Anaesthesiol Clin Pharmacol **31**, 308–316, doi:10.4103/0970-9185.161664 (2015).
10. Lukomska, B. *et al.* Challenges and Controversies in Human Mesenchymal Stem Cell Therapy. *Stem Cells Int* 2019, 9628536, doi:10.1155/2019/9628536 (2019).
11. Pati, S. & Rasmussen, T. E. Cellular therapies in trauma and critical care medicine: Looking towards the future. PLoS Med **14**, e1002343, doi:10.1371/journal.pmed.1002343 (2017).
12. Murphy, M. B., Moncivais, K. & Caplan, A. I. Mesenchymal stem cells: environmentally responsive therapeutics for regenerative medicine. Exp Mol Med **45**, e54, doi:10.1038/emm.2013.94 (2013).
13. Prockop, D. J. & Oh, J. Y. Medical therapies with adult stem/progenitor cells (MSCs): a backward journey from dramatic results in vivo to the cellular and molecular explanations. J Cell Biochem **113**, 1460–1469, doi:10.1002/jcb.24046 (2012).
14. Wang, X. *et al.* Adipose stem cells-conditioned medium blocks 6-hydroxydopamine-induced neurotoxicity via the IGF-1/PI3K/AKT pathway. Neurosci Lett **581**, 98–102, doi:10.1016/j.neulet.2014.08.033 (2014).
15. Zhang, Y. *et al.* Effect of exosomes derived from multipluripotent mesenchymal stromal cells on functional recovery and neurovascular plasticity in rats after traumatic brain injury. J Neurosurg **122**, 856–867, doi:10.3171/2014.11.JNS14770 (2015).
16. Vallabhaneni, K. C. *et al.* Extracellular vesicles from bone marrow mesenchymal stem/stromal cells transport tumor regulatory microRNA, proteins, and metabolites. Oncotarget **6**, 4953–4967, doi:10.18632/oncotarget.3211 (2015).
17. Kang, S. K. *et al.* Improvement of neurological deficits by intracerebral transplantation of human adipose tissue-derived stromal cells after cerebral ischemia in rats. Exp Neurol **183**, 355–366, doi:10.1016/s0014-4886(03)00089-x (2003).

18. Zhang, S. *et al.* Comparison of the therapeutic effects of human and mouse adipose-derived stem cells in a murine model of lipopolysaccharide-induced acute lung injury. Stem Cell Res Ther **4**, 13, doi:10.1186/scrt161 (2013).
19. Banas, A. *et al.* IFATS collection: in vivo therapeutic potential of human adipose tissue mesenchymal stem cells after transplantation into mice with liver injury. Stem Cells **26**, 2705–2712, doi:10.1634/stemcells.2008-0034 (2008).
20. Chen, Y. T. *et al.* Adipose-derived mesenchymal stem cell protects kidneys against ischemia-reperfusion injury through suppressing oxidative stress and inflammatory reaction. J Transl Med **9**, 51, doi:10.1186/1479-5876-9-51 (2011).
21. Tajiri, N. *et al.* Intravenous transplants of human adipose-derived stem cell protect the brain from traumatic brain injury-induced neurodegeneration and motor and cognitive impairments: cell graft biodistribution and soluble factors in young and aged rats. J Neurosci **34**, 313–326, doi:10.1523/JNEUROSCI.2425-13.2014 (2014).
22. Wei, X. *et al.* IFATS collection: The conditioned media of adipose stromal cells protect against hypoxia-ischemia-induced brain damage in neonatal rats. Stem Cells **27**, 478–488, doi:10.1634/stemcells.2008-0333 (2009).
23. Wei, X. *et al.* Adipose stromal cells-secreted neuroprotective media against neuronal apoptosis. Neurosci Lett **462**, 76–79, doi:10.1016/j.neulet.2009.06.054 (2009).
24. Marmarou, A. *et al.* A new model of diffuse brain injury in rats. Part I: Pathophysiology and biomechanics. J Neurosurg **80**, 291–300, doi:10.3171/jns.1994.80.2.0291 (1994).
25. Diehl, K. H. *et al.* A good practice guide to the administration of substances and removal of blood, including routes and volumes. J Appl Toxicol **21**, 15–23, doi:10.1002/jat.727 (2001).
26. Leibowitz, A. *et al.* Treatment of combined traumatic brain injury and hemorrhagic shock with fractionated blood products versus fresh whole blood in a rat model. Eur J Trauma Emerg Surg **45**, 263–271, doi:10.1007/s00068-018-0908-9 (2019).
27. Qi, L. *et al.* Ghrelin attenuates brain injury after traumatic brain injury and uncontrolled hemorrhagic shock in rats. Mol Med **18**, 186–193, doi:10.2119/molmed.2011.00390 (2012).
28. Johnstone B. *et al.* Abstract 133: Effectiveness of a Stem Cell-derived Therapeutic Factor Concentrate in a Mouse Embolic Stroke Model. Stroke. 2017;48(suppl_1):A133-A133.
29. Qi, L. *et al.* Ghrelin protects rats against traumatic brain injury and hemorrhagic shock through upregulation of UCP2. Ann Surg **260**, 169–178, doi:10.1097/SLA.0000000000000328 (2014).
30. Sled, J. G., Zijdenbos, A. P. & Evans, A. C. A nonparametric method for automatic correction of intensity nonuniformity in MRI data. IEEE Trans Med Imaging **17**, 87–97, doi:10.1109/42.668698 (1998).
31. Lau, J. C. *et al.* Longitudinal neuroanatomical changes determined by deformation-based morphometry in a mouse model of Alzheimer's disease. Neuroimage **42**, 19–27, doi:10.1016/j.neuroimage.2008.04.252 (2008).

32. Fonov, V. *et al.* Unbiased average age-appropriate atlases for pediatric studies. Neuroimage **54**, 313–327, doi:10.1016/j.neuroimage.2010.07.033 (2011).
33. Grand'maison, M. *et al.* Early cortical thickness changes predict beta-amyloid deposition in a mouse model of Alzheimer's disease. Neurobiol Dis **54**, 59–67, doi:10.1016/j.nbd.2013.02.005 (2013).
34. Hebert, F. *et al.* Cortical atrophy and hypoperfusion in a transgenic mouse model of Alzheimer's disease. Neurobiol Aging **34**, 1644–1652, doi:10.1016/j.neurobiolaging.2012.11.022 (2013).
35. Zehntner, S. P., Chakravarty, M. M., Bolovan, R. J., Chan, C. & Bedell, B. J. Synergistic tissue counterstaining and image segmentation techniques for accurate, quantitative immunohistochemistry. J Histochem Cytochem **56**, 873–880, doi:10.1369/jhc.2008.950345 (2008).
36. Ronn, T., Lendemans, S., de Groot, H. & Petrat, F. A new model of severe hemorrhagic shock in rats. Comp Med **61**, 419–426 (2011).
37. Benson, R. R. *et al.* Detection of hemorrhagic and axonal pathology in mild traumatic brain injury using advanced MRI: implications for neurorehabilitation. NeuroRehabilitation **31**, 261–279, doi:10.3233/NRE-2012-0795 (2012).
38. Hanks, R. *et al.* The relation between cognitive dysfunction and diffusion tensor imaging parameters in traumatic brain injury. Brain Inj **33**, 355–363, doi:10.1080/02699052.2018.1553073 (2019).
39. Sofroniew, M. V. Astrogliosis. Cold Spring Harb Perspect Biol **7**, a020420, doi:10.1101/cshperspect.a020420 (2014).
40. Li, S. *et al.* Temporal profiles of axonal injury following impact acceleration traumatic brain injury in rats–a comparative study with diffusion tensor imaging and morphological analysis. Int J Legal Med **127**, 159–167, doi:10.1007/s00414-012-0712-8 (2013).
41. Roland, J. L. *et al.* On the role of the corpus callosum in interhemispheric functional connectivity in humans. Proc Natl Acad Sci U S A **114**, 13278–13283, doi:10.1073/pnas.1707050114 (2017).
42. Wible, C. G. Hippocampal physiology, structure and function and the neuroscience of schizophrenia: a unified account of declarative memory deficits, working memory deficits and schizophrenic symptoms. Behav Sci (Basel) **3**, 298–315, doi:10.3390/bs3020298 (2013).
43. Xu, C. *et al.* Intravenously Infusing the Secretome of Adipose-Derived Mesenchymal Stem Cells Ameliorates Neuroinflammation and Neurological Functioning After Traumatic Brain Injury. Stem Cells Dev **29**, 222–234, doi:10.1089/scd.2019.0173 (2020).
44. Jha, K. A. *et al.* TSG-6 in conditioned media from adipose mesenchymal stem cells protects against visual deficits in mild traumatic brain injury model through neurovascular modulation. Stem Cell Res Ther **10**, 318, doi:10.1186/s13287-019-1436-1 (2019).

Figures

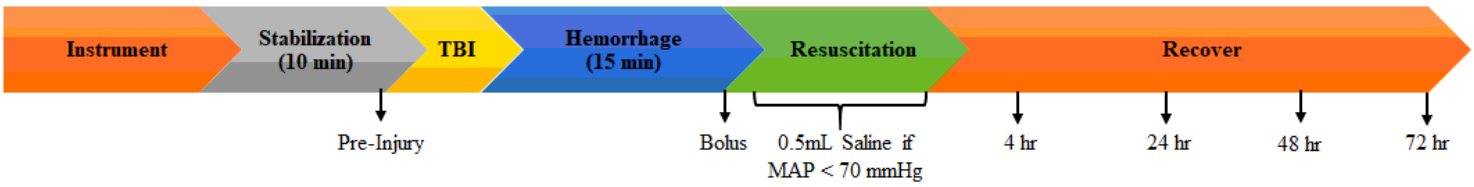

Figure 1

Injury timeline. Instrumentation was followed by 10 minutes of stabilization, at the end of which pre-injury vitals were recorded (Supplemental 1). The TBI was completed, followed by the 35% volume controlled hemorrhage. Resuscitation began with a bolus of T-101 or the vehicle control and 0.5mL saline was infused at 0.1ml/min if the MAP remained below 70 mmHg for five minutes. Then, cannulated vessels were ligated, catheters were removed, and the rat was recovered until end-points at four, 24, 48, or 72 hours after the start of hemorrhage.

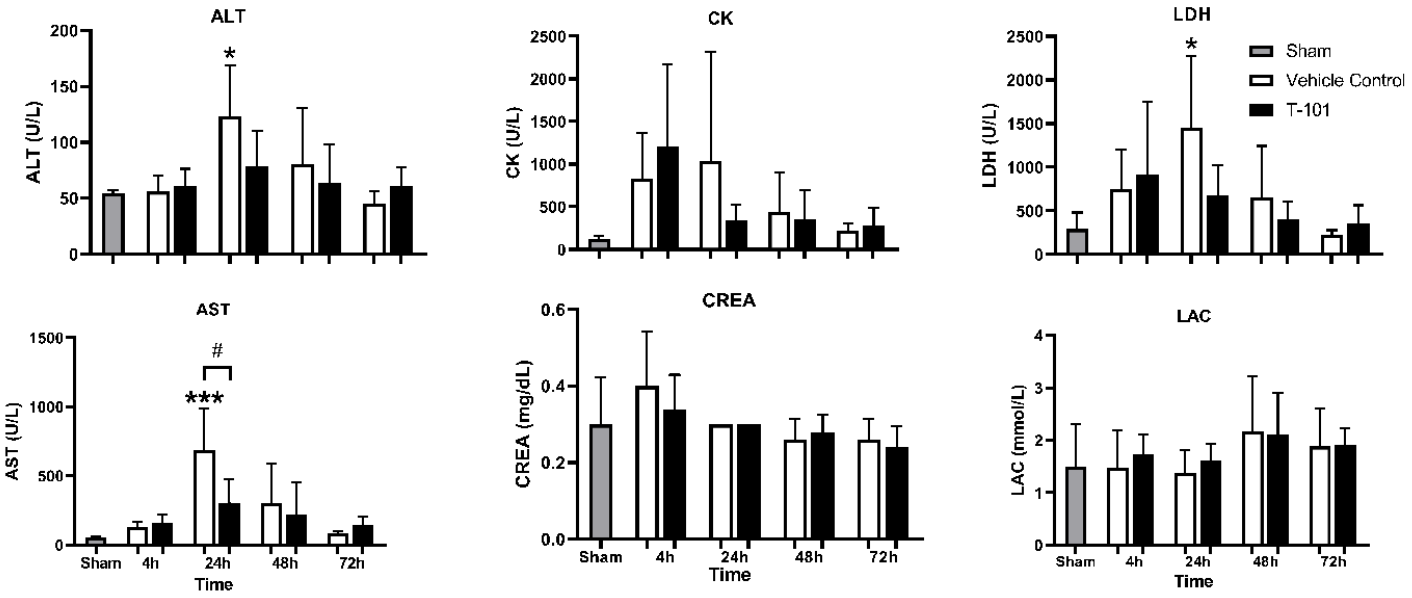

Figure 2

Blood chemistry analyses of plasma markers ALT, AST, CK, CREA, LDH and LAC. Data are plotted as the mean ± standard deviation. Significant differences for the vehicle control and T-101 groups when compared to the Sham group are noted by an asterisk (*P<0.05, ***P<0.0005). Significant difference between the vehicle control and T-101 groups is noted by # (P<0.05). Data compared by One Way ANOVA and Bonferroni's multiple comparison test.

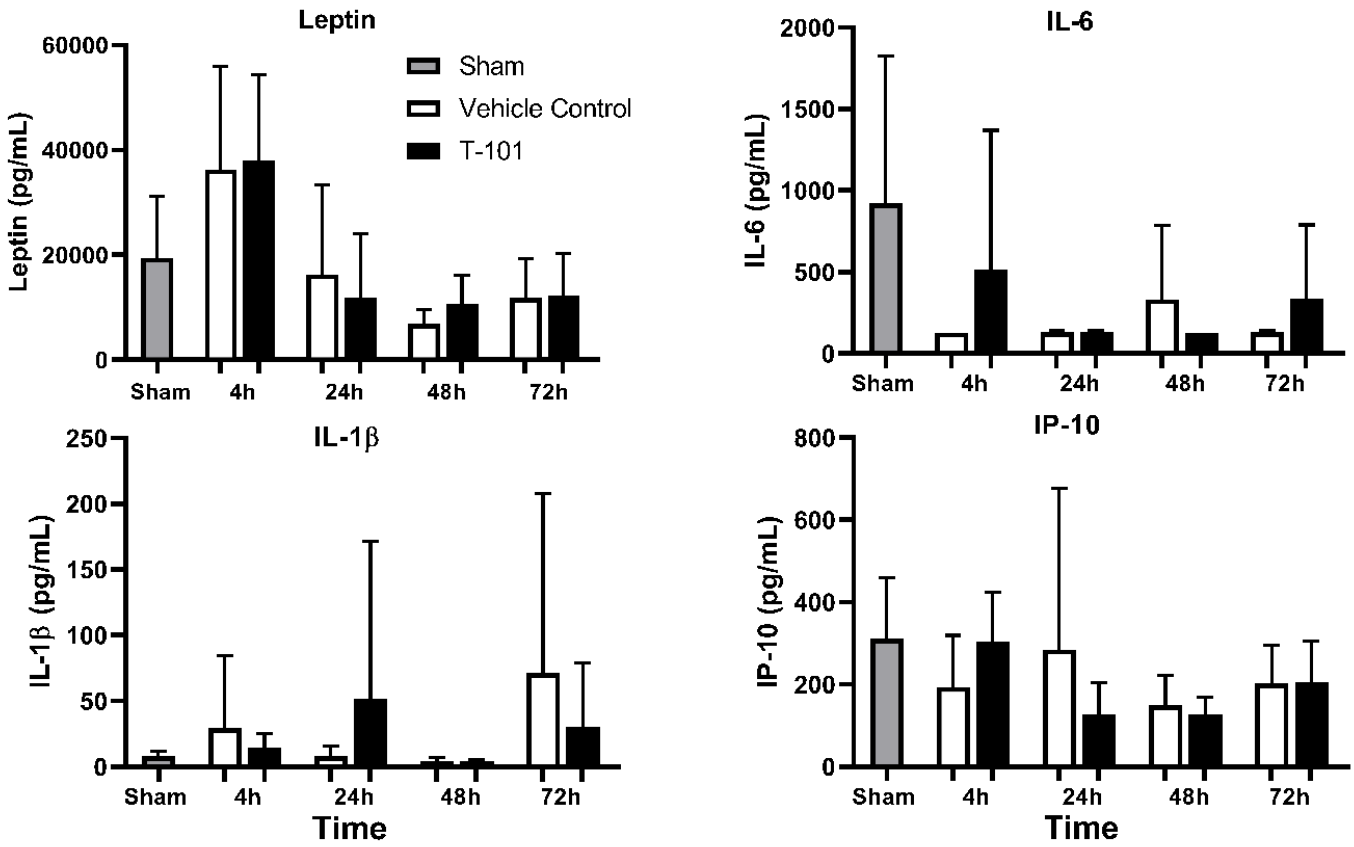

Figure 3

Systemic inflammation. Levels of leptin, IL-6, IL-1β, and IP-10 were quantified from blood plasma collected for the Sham group and injury groups at four, 24, 48, and 72 hours. Data are plotted as the mean ± standard deviation. There were no significant differences. Data compared by One Way ANOVA and Bonferroni's multiple comparison test.

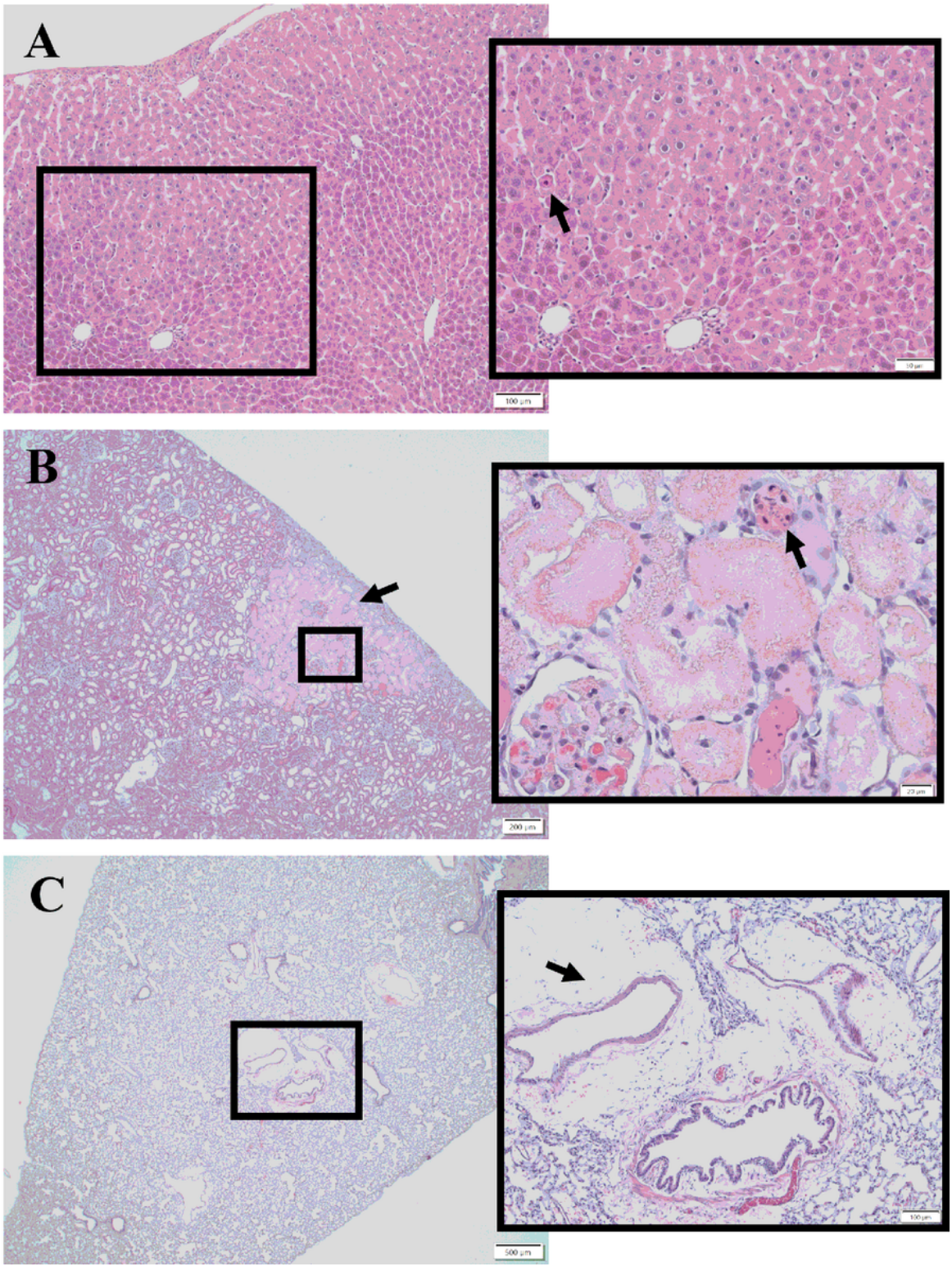

Figure 4

H&E Histology Images. Representative images show histological findings in the (A) liver, (B) kidney, and (C) lung. Hepatocellular degeneration was observed in the liver with an arrow pointing to a necrotic hepatocyte in the vehicle control group (A). A focally extensive area of necrosis is indicated by the arrow. Renal tubular coagulative necrosis and rare lytic necrosis were observed as shown in the inset from the vehicle control group (B). Additional observations included intratubular casts of mucoprotien and

glomerulus with marked mesangial and endocapillary fibrin, edema, and congestions admixed with increased hypercellularity, which is indicative of glomerulonephritis. Perivascular and vascular changes were observed in the lung for both groups and the image is from the T-101 group (C). The arrow points to mild to moderate multifocal perivascular edema. The inset shows one bronchiole and several large arterioles with moderate perivascular edema. Scale bars = 100μm, 50μm; (B) 200μm, 20μm; (C) 500μm, 100μm.

Figure 5

Diffusion tensor imaging (DTI) Fractional Anisotropy (FA) variation in brain regions. The greatest changes in FA were observed in the corpus callosum and the fimbria while there were no significant changes in the cortex or hippocampus. Data are plotted as the mean ± standard deviation with significant differences from Sham for the vehicle control and T-101 noted by asterisks (** P<0.005, *** P<0.0005) and differences between injury groups for a given time-point are noted by the pound sign (#, P<0.05); Data compared by One Way ANOVA and Bonferroni's multiple comparison test.

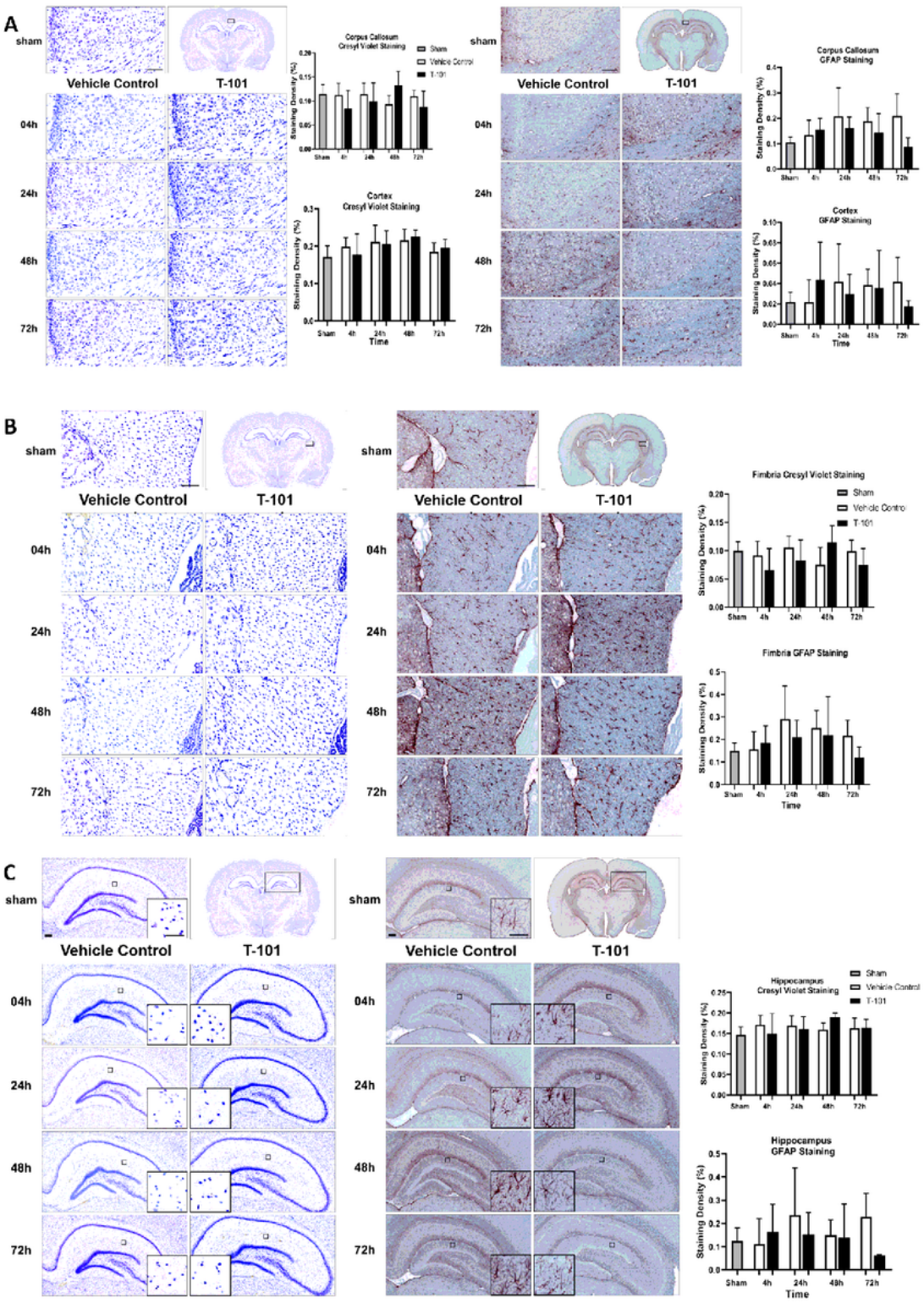

Figure 6

Brain immunohistochemistry. The (A) corpus callosum and cortex, (B) fimbria, and (C) hippocampus were stained with Cresyl Violet (left) for the Nissl substance in neurons and GFAP (right) for astrocytes. Data are plotted as the mean ± standard deviation; no significant differences between the SHAM and injury groups. Scale bar equals 100μm.

Supplementary Files

This is a list of supplementary files associated with this preprint. Click to download.

- Supplemental1Vitals.docx
- Supplemental2Pathology.docx